Design and structural analysis of a thrust chamber for a spinning supersonic rocket – a case study

K. M. Rajan
Armament Research and Development Establishment
Pune, India

K. Narasimhan
Department of Metallurgical Engineering. and Materials Science
Indian Institute of Technology
Mumbai, India

ABSTRACT

The design of a thrust chamber for a rocket propulsion system is a challenging task. The thrust chamber has to be designed for minimum structural weight with an adequate factor of safety. This calls for a thorough knowledge of various structural loads, both internal and external, and the behaviour of the structure in flight. This paper presents the design and structural analysis of a pressure vessel used as thrust chamber for a rocket propulsion unit. The effects of kinetic heating, thermal stress, spinning and various aerodynamic loads and their mutual interactions are accounted for in this analysis. Based on a detailed stress analysis of the components and a modal/structural dynamic analysis of the flight vehicle as a whole, in which the thrust chamber is the main load bearing member, the required mechanical properties of the thrust chamber are obtained.

NOMENCLATURE

A	area
a	inner radius
b	outer radius
[Bij]	row vector of the geometric matrix [B] in the beginning
G	centre of gravity
CP	centre of pressure
C_p	specific heat of gas at constant pressure
C_{ps}	specific heat of the skin material (kJ/kg K)
d	internal diameter of thrust chambeer
Fa	axial force
Fai	inertia force in axial direction
F_D	drag force
F_{LN}	nose lift
F_{TL}	tail lift
F_T	thrust
Fvi	inertial load in transverse direction
FEM	finite elements method
g	acceleration due to gravity, m/s^2
G	$Cps.tp.\rho$
h_g	heat transfer coefficient (kJ/m^2 K)
k_g	thermal conductivity of gas
k	thermal conductivity of case material (kJ/m^2K)
K_m	stiffness matrix
$K_G u$	centrifugal force field contribution
M_n	free stream Mach number
p	internal pressure
q	heat due to radiation
r	radius of the thrust chamber
R_b	actual bending stress/allowable bending stress
R_c	actual compressive stress/allowable compressive stress
R · F	recovery factor
R_s	actual shear stress/allowable shear stress
t_p	skin thickness (m)
T	free stream static temperature
Ta	torsional load
Tai	inertial torsional load
Tw	Wall temperature (K)
u	displacement matrix
$\ddot{U}$	acceleration
U_0	maximum displacement
σ_x	longitudinal stress
σ_y	hoop stress
τ_{xy}	torsional stress
γ	ratio of specific heat of air at constant pressure (C_p) and at constant volume (C_v)

Paper No. 2688. Manuscript received 19 June 2001 revised version received 7 July 2002, accepted 22 February 2005.

ρ density of the skin material (kg/m^3)
Ω spin rate
ω angular velocity
$2M\Omega u$ Corriolis acceleration contribution
$M\Omega\Omega u$ centripetal acceleration contribution
μ absolute gas viscosity
v free steam velociy (m/s)
w mass of unit area of tube wall

1.0 INTRODUCTION

It is the primary responsibility of a design engineer to design a specific component or a system to ensure design adequacy, selection of the basic raw material and suitable manufacturing process to ensure improved performance and reliability in a most competitive way. To achieve these goals the design engineer should have a clear understanding of the critical role the subject component/store has to play, the magnitude and nature of various forces acting on the component and the design constraints offered by the functional and assembly requirements of the store. It is also pertinent to have well-defined input parameters.

2.0 OBJECTIVES

The primary objective of this work is to design a pressure vessel for a critical application with high specific strength, close dimensional tolerances and very low surface roughness in a cost-effective way. This pressure vessel is a thrust chamber of a rocket propulsion system and has to function very reliably without any performance degradation under static and dynamic loading conditions and in extreme climatic conditions.

The external diameter of the thrust chamber is restricted to 206mm as the rocket was decided to be launched through a readily available launcher tube. The aerodynamic loads acting on the rocket along its flight trajectory were estimated using a six degree of freedom computer code. The thrust chamber is to be designed primarily as a pressure vessel. It is to be followed by a detailed structural analysis of the rocket to ensure the structural integrity of the rocket in flight. The stress analysis has been done for the pressure vessel based on maximum distortion energy theory. The major subsystems of a typical rocket are shown in Fig. 1.

3.0 LOADS ACTING ON A TYPICAL ROCKET

Generally a spinning rocket is launched through a launcher tube. After the rocket is ignited, before it leaves the launcher tube, the thrust chamber of the rocket experiences high pressure due to the propellant combustion gases. Since the thrust chamber is normally internally insulated, the thermal stress experienced by the thrust chamber material is negligible. However, if there is a considerable temperature gradient across the skin temperature, the magnitude of the thermal stress will be considerable.

When the rocket in flight is following a pre- determined trajectory, aerodynamic lift forces are produced by the nose and stabilisation units of the rocket. The flight vehicle is subjected to aerodynamic bending moments, inertia forces and drag force. The internal pressure continues to act in the thrust chamber during the boost phase till the end of propellant burning. In order to minimise the effect of thrust misalignment and subsequent increase in dispersion of the rocket from its desired trajectory, the rocket is provided with spin throughout its trajectory. This imparted spin increases with increase in linear velocity of the rocket and produces centrifugal stresses and torsional stresses in the rocket body whose section modulus varies along its length. A schematic diagram of the rocket in equilibrium under the application of various loads is shown in Fig. 2.

For achieving a specified range for a given payload, the total energy requirement (total impulse) and hence the type and the mass of propellant required are worked out from the fundamentals of rocket propulsion[1]. From this total energy requirement, the thrust-time and pressure-time curves required for the mission requirements are obtained. For a detailed understanding of the methodology of these calculations, the reader may refer the book on 'Rocket Propulsion Elements' by Sutton[1].

4.0 STATIC STRESS ANALYSIS

The rocket thrust chamber when fired in static firing mode experiences internal pressure. The pressure-time curve required to meet the total energy requirement for the rocket under study is shown in Fig. 3.

Maximum internal pressure 'P' acting in the thrust chamber (ref. Fig. 3) = 14MPa.

For the pressure vessel, hoop stress $\sigma_y = \dfrac{pd}{2t_p}$ . . . (1)

= 660MPa

Longitudinal stress due to pressure, $\sigma_x = \dfrac{pd}{4t_p}$ . . . (2)

= 330MPa

where, $d = 0{\cdot}202$m and $t_p = 0{\cdot}002$m

4.1 Thermal analysis

Thermal analysis of the combustion chamber is a transient heat transfer problem. The thermal analysis was performed based on a finite difference method[1].

Heat transfer coefficient for the propellant combustion gas was calculated using the Equation[1],

$$\frac{h_g \cdot d}{k_g} = 0{\cdot}026\left(\frac{d \cdot v \cdot \rho_g}{\mu \cdot g}\right)^{0{\cdot}8}\left(\frac{\mu \cdot g \cdot C_p}{k_g}\right)^{0{\cdot}4} \quad \ldots (3)$$

From the above Equation (3), h_g works out to be approximately equal to 147W/m^2 °C

A computer program was developed for this iterative process. The thermal analysis shows the maximum temperature rise attained by the thrust chamber material is quite low as shown in Fig. 4. Hence, the thermal stress developed in the thrust chamber material is neglected.

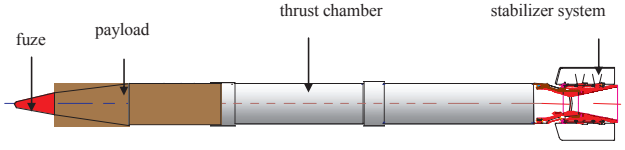

Figure 1. A schematic diagram of the rocket.

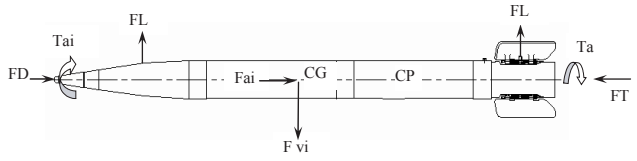

Figure 2. A schematic loading diagram of the system in equilibrium.

https://doi.org/10.1017/S0001924000000701 Published online by Cambridge University Press

4.2 Estimation of strength requirement of thrust chamber in static firing mode

The equivalent von Mises stress acting on the thrust chamber material is :

$$\sigma_{eq} = \sqrt{\sigma_1^2 + \sigma_2^2 - \sigma_1 \sigma_2} \quad \ldots (4)$$

$$= \sqrt{660^2 + 330^2 - 660 \times 330} = 576 \text{ MPa}$$

Generally, experimental results on ductile materials show the results to be close to the prediction based on distortion energy theory. The thrust chambers are manufactured in very large numbers and function very reliably under different flying conditions. They are assembled to other subsystems using threaded joints at either end. Weight optimisation of the thrust chamber is not considered in this case, as the weight of this component ,which is part of a free flight artillery rocket, is not mission critical, unlike the case of an aerospace vehicle. The factor of safety for the rocket thrust chamber has therefore been decided to be a minimum of 1·5.

Hence, the required yield strength or 0·2% proof stress (0·2% P.S) of the material is given by,

$$0{\cdot}2\%\ P.S = F.S. \times \sigma_{eq} \quad \ldots (5)$$
$$= 864\text{MPa}$$

A factor of safety (*F.S.*) of two on ultimate tensile strength (UTS) is considered in the present case, for the design of the free flight rocket.

$$\text{Hence, required UTS} = F.S. \times \sigma_{eq} \quad \ldots (6)$$
$$= 1{,}152\text{MPa}$$

5.0 DYNAMIC STRESS ANALYSIS

The dynamic mode refers to the condition when the rocket is flying in the air subjected to the various aerodynamic and inertia forces. The rocket body in the equilibrium condition is shown in Fig. 2.

5.1 Estimation of shear force and bending moment diagrams

The shear force and bending moment acting on the system in the dynamic mode are computed. The entire length of the rocket is divided into a convenient number of elements. The external vertical lift loads acting on the nose and stabiliser units and the inertia forces acting through each element of the rocket are considered. It acts as a beam with uniformly distributed loads and concentrated lift forces acting on each end of the rocket[2]. The shear force diagram thus constructed is shown in Fig. 5.

Taking bending moments about the center of gravity of the rocket, considering the effect of uniformly distributed inertia forces acting vertically down through all the elements and the aerodynamic lift forces acting at the nose and stabiliser systems of the rocket, the bending moment diagram for the rocket is calculated and is shown in Fig. 6.

The pressure vessel is located between the payload and the stabilisation unit of the flight vehicle as shown in Fig. 1. Hence, for the structural analysis of the pressure vessel, the maximum shear force and bending moment corresponding to this region are considered.

In the dynamic mode, when the rocket comes out of the launcher tube after about 200ms as designed, the internal chamber pressure drops down to 9MPa as can be seen from Fig. 3. Stresses due to internal pressure of 9MPa during dynamic mode are

hoop stress = 460MPa

longitudinal stress = 230MPa

For a thin walled pressure vessel, as given in reference[2],

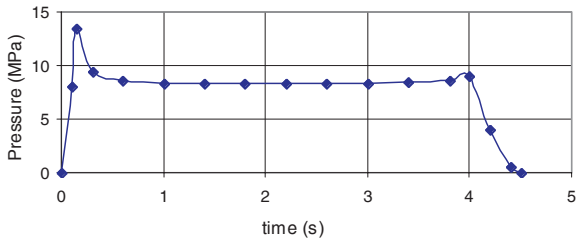

Figure 3. Theoretical pressure-time curve for the rocket thrust chamber.

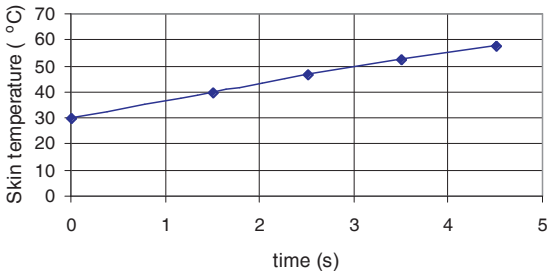

Figure 4. Transient temperature-time history of the thrust chamber of the rocket after four seconds.

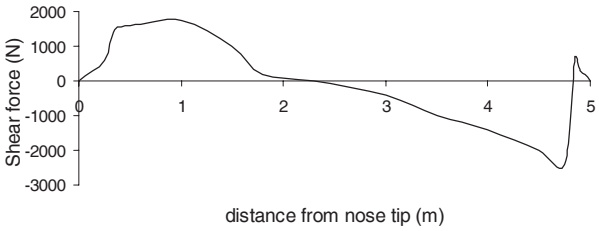

Figure 5. Shear force diagram with and without spin.

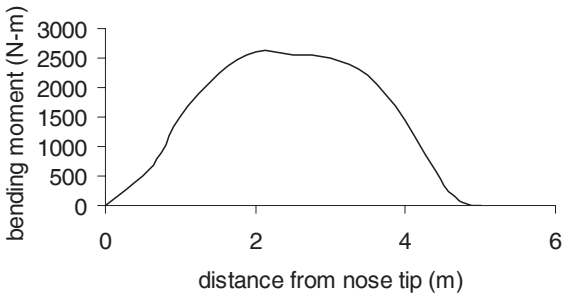

Figure 6. Bending moment diagram with and without spin.

https://doi.org/10.1017/S0001924000000701 Published online by Cambridge University Press

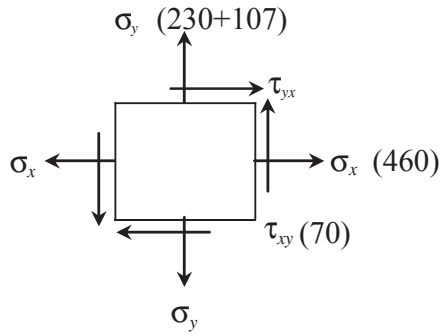

Figure 7. Stresses acting on an element of the thrust chamber.

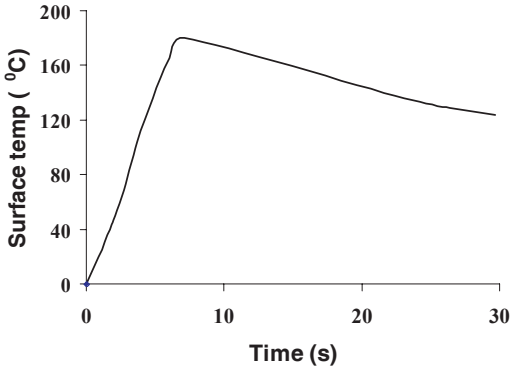

Figure 8. Temperature-time history of aerodynamic heating.

Bending moment, $= M = \sigma \times \pi \times r^2 \times t_p$ . . . (7)

Hence, bending stress due to aerodynamic lift loads, σ = 107MPa

Torque developed in the thrust chamber = 32·05Nm

Torque due to spin effect = $\tau_{sh} \times 2 \times \Pi \times r^2 \times t_p$

So, shear stress developed, T_{sh} = 70MPa

The various stresses acting on an element on the thrust chamber are shown in Fig. 7.

Hence, principal stresses acting on the pressure vessel are :

$$\sigma_{1,2} = \frac{\sigma_x + \sigma_y}{2} \pm \sqrt{\frac{(\sigma_x - \sigma_y)^2}{2} + \tau xy^2} = \frac{(460) + (230+107)}{2} \pm \sqrt{\left(\frac{460-337}{2}\right)^2 + 70^2} \quad \ldots (8)$$

So, principal stresses are:

σ_1 = 493MPa

σ_2 = 307MPa

Using the principal stresses, the resultant equivalent stress, acting on the body of the thrust chamber is calculated.

Equivalent von Mises stress,

$$\sigma_{eq} = \sqrt{\sigma_1^2 + \sigma_2^2 - \sigma_1 \sigma_2}$$

= 432MPa

Considering the same factor of safety used in the previous analysis of 1·5, the required strength in the flight mode is 648MPa (1·5*432MPa) only. Hence, it can be seen that the minimum 0·2% proof strength required for the thrust chamber is 864MPa and the ultimate tensile strength (UTS) is 1,152MPa.

5.2 Interactive equation for buckling

As can be seen from Fig. 2 the rocket and the pressure vessels are subjected to various loads like compressive stresses, bending stresses and torsional stresses. Hence the system has to be checked for buckling under the effect of these loads acting simultaneously.

The governing interactive equation for the combined action of these forces is given by Bruhn[3] and expressed as,

$$R_c + R_b + R_s^2 \le 1 \quad \ldots (9)$$

For this analysis the rocket at the burn out phase of the propellant in its trajectory is considered as the stiffness of the rocket structure corresponding to this state will be less compared to the condition when the thrust chamber is pressurised.

The axial critical compressive stress F_{cr} is estimated using Figs C8.7 of Ref. 3 and the equation for critical buckling load P_a is given by:

$$P_a = 2\pi r t_p F_{cr} \quad \ldots (10)$$

The critical bending stress F_{bcr} is estimated using Figs C8.12 of Ref. 3 for the given r/t*p* and l/t*p* of the thrust chamber. The equation for critical bending moment M_a is given by,

$$M_a = F_{bcr}\, \pi . r^2 . t_p \quad \ldots (11)$$

The critical torsional moment T_a is calculated using fig C8.18 of ref T and the critical shear stress *Fstcr* is calculated using the equation,

$$T_a = F_{stcr} \cdot 2 \cdot r^2 . t_p \quad \ldots (12)$$

Substituting the calculated values in Equation (9), we get,

$$R_c + R_b + R_s^2 = \frac{7 \cdot 8}{25 \cdot 63} + \frac{10 \cdot 76}{82 \cdot 8} + \frac{7^2}{14 \cdot 7^2} = 0 \cdot 66 < 1 \quad \ldots (13)$$

Hence the structure as a whole and the pressure vessel in particular are free from buckling under combined loading.

6.0 AERODYNAMIC HEATING

Aerodynamic heating results from the air flow about the surface of the rocket while the rocket is in flight due to friction of the air along the surface of the rocket and compression at and near the stagnation regions of the flight vehicle. In this process, a portion of the kinetic energy of the air is converted into thermal energy within the boundary layer of the rocket.

The final or stagnation temperature T_o is given by,

$$T_o = T\left[1 + \frac{\gamma - 1}{2} M_n^2\right]$$

Equation (13) is applicable for a compressible non-heat conducting gas. Since there is a small amount of heat transfer within the boundary layer, 'recovery temperature, T_R' differs from the stagnation temperature and is expressed as,

$$T_R = T\left[1 + RF \cdot \frac{\gamma - 1}{2} M_n^2\right] \quad \ldots (14)$$

Where,

$$RF = \frac{T_r - T}{T_o - T} \quad \ldots (15)$$

The value of T_R varies from 0·85 for laminar flow to 0·88 for turbulent flow. The governing equation for the aerodynamic heating is given by Ref. 2,

$$G \cdot \frac{dT_w}{dt} = h(T_R - T_w) + q \quad \ldots (16)$$

https://doi.org/10.1017/S0001924000000701 Published online by Cambridge University Press

The material parameters used for the aerodynamic heating study are:

material – AISI 4130 steel
C_p = 0·452kJ/kg C
density = 7,860kg/m^3
thickness = 0·002m

The heating effect due to turbulent air stream outside the pressure vessel was computed using Equation (16). The maximum computed temperature is about 180°C. The reduction in tensile strength over an exposure period of about 10 seconds at 180°C during the flight is negligible. The pressure vessel skin temperature versus time history is plotted in Fig. 8. However, a maximum reduction in strength of about 0·4% is accounted for in the design by specifying a marginally higher 0·2% proof stress and ultimate tensile strength than required by stress analysis results.

Hence, the 0·2% proof stress required for the thrust chamber = 900MPa The ultimate tensile strength required for the thrust chamber = 1,200MPa

7.0 MODAL ANALYSIS

The dynamic characteristics of a projectile are to be studied to predict its behaviour in flight. This knowledge is fundamental for the analysis of very slender supersonic flight vehicles to prevent aero elastic instability.

A modal analysis has been carried out by idealising the rocket structure by a 2D finite element model using beam elements. Master degrees of freedoms (MDOF) are selected at locations with large mass to stiffness ratio and regions where displacements are to be monitored. The idealised finite element model of the flight vehicle with boundary conditions for transverse vibration is shown in Fig. 9 and the first three natural frequencies and their corresponding mode shapes in Fig. 10 respectively.

7.1 Modal analysis considering the effect of joint flexibility and spin

The analysis of spinning structures differ from that of stationary structures due to the complexity of acceleration which acts throughout the system. In addition to the acceleration resulting from the elastic structural deformation, contributions due to Corriolis and centripetal accelerations may be of significance.

The introduction of joints in the structure reduces the overall stiffness and thereby increases the flexibility[4]. Different methods are available for estimating Joint rotation constant (JRC)[5,6]. Modal analysis has been carried out for the structure considering the joint flexibility by estimating the Joint rotation constant (JRC) at the joints. Based on Ref. 6 for a category of good joints from the graph (see Fig. 2) for a known thrust chamber nominal diameter of 206mm, the joint rotation constant is obtained as $1{\cdot}0 \times 10^{-7}$ rad/(N-m). The analysis results are shown in Table (1). It shows marginal reduction in natural frequencies due to joint flexibility effect.

The introduction of spin includes centripetal acceleration, Corriolis accelerations and modification of structural stiffness due to spin-induced loads on the structure. As a result the free vibration problem is modified to (7-9):

$$M\ddot{U} + 2M\bar{\Omega}\dot{U}(K + K_G + M\bar{\Omega}\bar{\Omega})u = 0 \quad \ldots (17)$$

Rotating bodies are subjected to stress stiffening and spin softening which account for the changes that occur in the plane of the spinning structure. Spinning bodies tend to be not as stiff as predicted by stress stiffening alone. Spin softening or centrifugal softening accounts for the geometry changes that occur in the plane of rotation of a spinning body. This is different from stress stiffening and is a higher order effect. Only vibration modes which are in the plane of spin are affected.

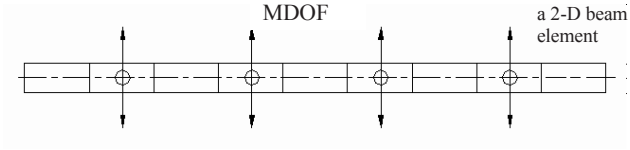

Figure 9. Idealised finite element beam model of rocket for modal analysis.

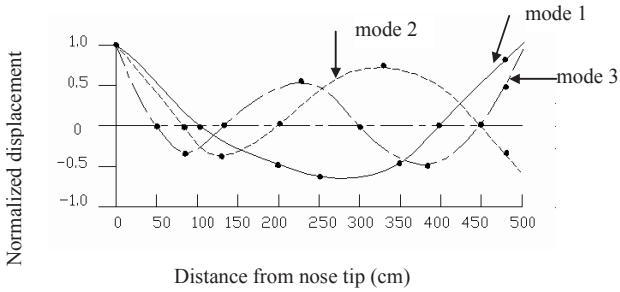

Figure 10. Natural frequencies and corresponding mode shapes.

Modal analysis was carried out using CSA/NASTRAN finite elements analysis software. The modal analysis results considering the effects of stress stiffening and spin softening are presented in Table (1) and the first two mode shapes are shown in Fig. 12 and Fig. 13 respectively.

It is seen from the above analyses that there exists sufficient separation between the structural frequencies (first mode frequency = 16Hz) and the roll frequency (22Hz) of the flight vehicle. Hence the material properties and the thrust chamber dimensions assumed for the design of the thrust chamber are acceptable.

Hence, from the above detailed stress analyses, the pressure vessel material strength properties required are:

0·2% proof strength = 900MPa (minimum)
Ultimate tensile strength = 1,200MPa (minimum)

8.0 CONCLUSIONS

Through a detailed stress analysis of the pressure vessel as a component and structural dynamic analysis of the system in which the pressure vessel is the main load-bearing member, the minimum mechanical property requirements of the pressure vessel to be developed are obtained (0·2% proof stress = 900MPa, ultimate tensile strength = 1,200MPa). Apart from the high mechanical

Table 1
Effect of joint flexibility and spin rate on natural frequencies

Sl.No.	Analysis option	Mode 1	Mode 2	Mode 3
1	Natural frequency without JRC and with out spin (Hz)	30	78	171
2	Natural frequency with) JRC and with out spin (Hz	29·5	77	168
3	Natural frequency with stress stiffening (Hz)	33	85	182
4	Natural frequency with stress stiffening and spin softening (Hz)	16	67	165

https://doi.org/10.1017/S0001924000000701 Published online by Cambridge University Press

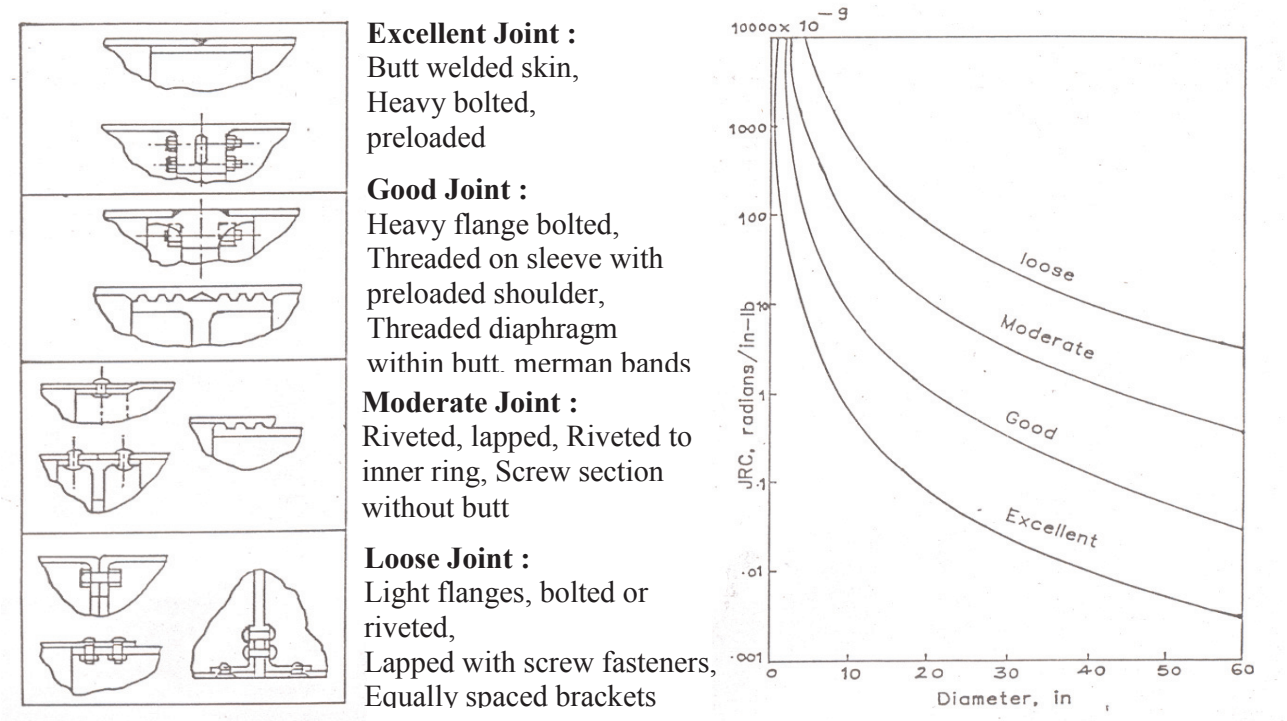

Figure 11. Joint rotation constants[6].

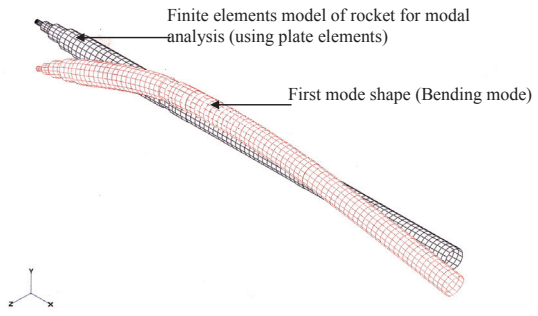

Figure 12. First mode shape of rocket with spin (1300rpm).

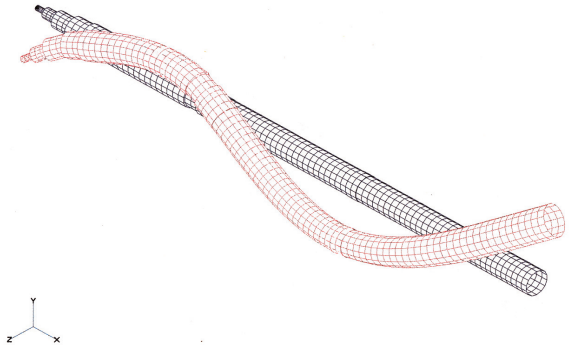

Figure 13. Second mode shape of rocket with spin (1300rpm).

property requirements, close dimensional tolerances and minimum mass unbalance are equally important considerations for the effective performance of the pressure vessel as a thrust chamber. The manufacturing technique adopted for the fabrication of the pressure vessel should meet all these challenging requirements.

REFERENCES

1. SUTTON, G.P. and ROSS, D.M. *Rocket Propulsion Elements*, 4th Ed, John Wiley and Sons, 1976, New York.
2. CHIN, S.S. *Missile Configuration Design*, McGraw-Hill Book Company, 1961, USA.
3. BRUHN, E. F. *Analysis and design of flight vehicle structures*, Tri-State Offset Company, 1973, USA.
4. HURTLY, W.C. and RUBINSTEIN, M.F. *Dynamics of Structures*, Printice Hall of India Pvt, 1967, New Delhi.
5. PANDEY, D.S., SRINIVASAN, K., NAIDU, V.V. and VIDYASAGAR, K. Structural testing – a review for applications to missile systems, ICSTAD Proceedings, **3**, 29 July–3 August, 1990, Bangalore, India, pp 1200-1201.
6. VERNER, L.A. and SUMNER, A.L. Prediction and measurement of natural vibrations of multistage launch vehicles, *AIAA J*, January 1963, **1**, (2), p 377.
7. LIKINS, P.W., BARBERA, F.J. and BULDELEY, V. Mathematical modelling of spinning elastic bodies for modal analysis, *AIAA J*, September 1973, **11**, (9), pp 1257-1258.
8. LAURENSON, R.M. Modal analysis of rotating flexible structures, *AIAA J*, October 1976, **14**, (1), pp 1444-1450.
9. ZOHAR, A. and ABOUNDI, J. Free vibration of thin circular finite rotating cylinder, 1973, *J Mech. Sciences*, **15**, pp 260-278.

https://doi.org/10.1017/S0001924000000701 Published online by Cambridge University Press